DOI: 10.13009/EUCASS2019-950

Study on Aerodynamic Stability of a Deployable Aerobraking Re-entry Capsule

Alessandro Zamprotta, Alberto Fedele**, Stefano Mungiguerra*, Raffaele Savino**
**University of Naples Federico II*
alessandro.zamprotta@studenti.unina.it, stefano.mungiguerra@unina.it, rasavino@unina.it
***CIRA, Italian Aerospace Research Centre*
a.fedele@cira.it

Abstract
Atmospheric re-entry capsules suffer dynamic instabilities, resulting in undamped aerodynamic pitching oscillations. The aim of this work is the characterization of the dynamic stability of a capsule with a 45° sphere-cone deployable heat shield by applying the forced-oscillation method through Computational Fluid Dynamics. Results have been analysed to investigate the influence of Mach number and oscillation amplitude, revealing a peak of instability in the transonic regime, enhanced at low amplitude. The predicted pitching behaviour has been compared with the available data of similar shape capsules in literature, showing a reasonably good agreement.

1. Introduction

With the emergence of microsatellite launch vehicle technology and the development of interest in space commercialization, there is a renewed need for innovative entry vehicle technology to return mass from Low Earth Orbit. Atmospheric re-entry refers to the entering in the Earth atmosphere, or other planets, of an object or a space vehicle and it is one of the most critical phases of a space mission. This is due to the strong inertial and thermal loads which affect the capsule because of the high speed reached during the re-entry phase. The presence of the atmosphere allows the reduction of the vehicle velocity down to landing values, even though it imposes complex ballistic, aerodynamic and thermal protection design solutions. Numerous system studies in the past sixty years demonstrate the benefit of developing a new decelerator technology capable of operating at higher Mach numbers and higher dynamic pressures than existing decelerators allow. In order to achieve this goal, scientists put their attention at the ballistic coefficient (usually designated with the Greek symbol "β"). This coefficient is a function of the mass M of the vehicle, the cross-section area S and the drag coefficient CD, see equation (1).

$$\beta = \frac{M}{C_D S} \tag{1}$$

Vehicles with a low ballistic coefficient experience most of their deceleration in the thin upper atmosphere. They take longer to slow down and generate less heat but experience this heat over a longer period. The ballistic coefficient significantly affects the nature of the re-entry profile, in terms of heating and trajectory [1]. Figure 1 shows the effect of β on maximum heating rate and maximum dynamic pressure. As one can notice, the peak heating rate drops markedly as β decreases below 1000 Pa, the maximum dynamic pressure is linear with it, with a slope fixed by the spacecraft efficiency L/D. Hence, the ballistic coefficient is a significant parameter governing the peak heat shield temperature and decreasing it below 25 kg/m^2 a spacecraft would have a less demanding entry environment. Even so, the re-entry vehicles built so far were characterised by a constant value of the ballistic coefficient for the entire mission, since β is fixed by the geometry. Therefore, a new type of configuration is needed for the re-entry capsule, such that the ballistic coefficient can be treated as an independent parameter. Specifically, a capsule that is capable to have different geometry between launch and re-entry.

DOI: 10.13009/EUCASS2019-950

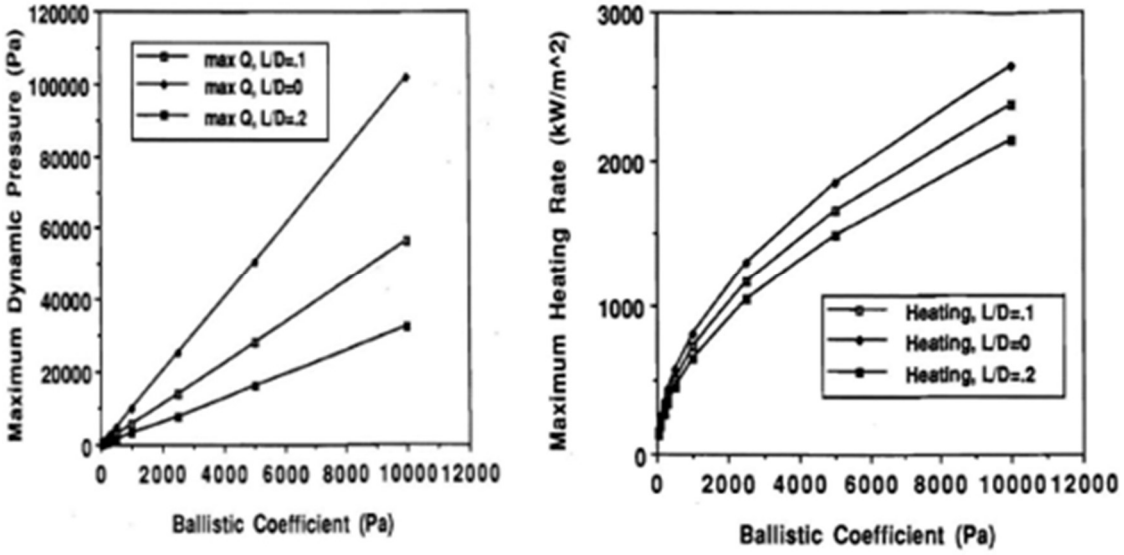

Figure 1: Maximum Dynamic Pressure (on the left) and Maximum Heating Rate (on the right) as a function of the ballistic coefficient [1].

Much effort is currently dedicated in the aerospace community to study systems with deployable heat shield for atmospheric re-entry to accomplish such goal [1, 2, 3, 4, 5]. However, it is well known in literature [6] that this kind of capsules suffer dynamic instabilities, resulting in undamped aerodynamic pitching oscillations, in particular in the transonic region. The dynamic behaviour of the capsule is an important issue that must be faced during the development of a re-entry capsule. In fact, the attitude of a capsule should be aligned along the velocity direction during the whole re-entry trajectory both to protect the payload and to ensure the deployment of the parachute. However, many capsules must maintain the attitude without any active control system and, therefore, only relying on their own aerodynamic stability. Since the centre of gravity of such vehicle is located forward of the centre of pressure the capsule is statically stable in general as it is the capsule chosen as reference for the present study and it is shown in [7] and [8]. However, dynamic stability shall not be taken for granted. In fact, most of the capsule geometries suffer dynamic instability in the transonic regime that could trigger a tumbling or an excessive oscillation that can be difficult to be recovered in the subsonic regime. Initial investigations into the phenomenon of dynamic stability as applied to blunt bodies began in the 1950s as the development of ballistic missile and space exploration technologies gained momentum. However, due the drastically different operational environments and geometries of entry vehicles, engineers lacked intuitive insight into the problem at the early stages. The studies that have been made during the years highlighted the unpredictable nature of blunt body dynamic stability, its sensitivity to geometric and environmental variables, and the difficulties associated with determining the stability parameters analytically, numerically, or experimentally. Wind tunnel experiments, free flight experiments and numerical investigations are the common techniques to examine the dynamic behaviour of aerospace vehicles. Because free flight experiments are costly and wind tunnel test campaign cannot always reproduce the exact flow condition, numerical investigations can be considered for preliminary dynamic analysis of hypersonic vehicles.
The aim of this work is to study the dynamic stability of a deployable re-entry capsule with a 45° sphere-cone [9], in order to have better knowledge of their dynamic behavior. According to the flow regime scenario shown in [9], the analyses will be performed in the continuum regime in specific points along the re-entry trajectory that have been chosen for their critical flow condition that affect negatively the dynamic stability as it will be shown in the following sections.

2. Method, study case and numerical model

2.1 Equations of motion

The motion of a space capsule during planetary re-entry can be described, by classical mechanics, as a combination of translation and rotation around its centre of gravity with six equations. Figure 2 [10] describes the coordinate system used for the formulation of the problem. A reduce set of equations of motion of the vehicle can be obtained using some assumptions: the displacement is made in the vertical plane, the rotation of the earth is neglected and the gravity force is constant.

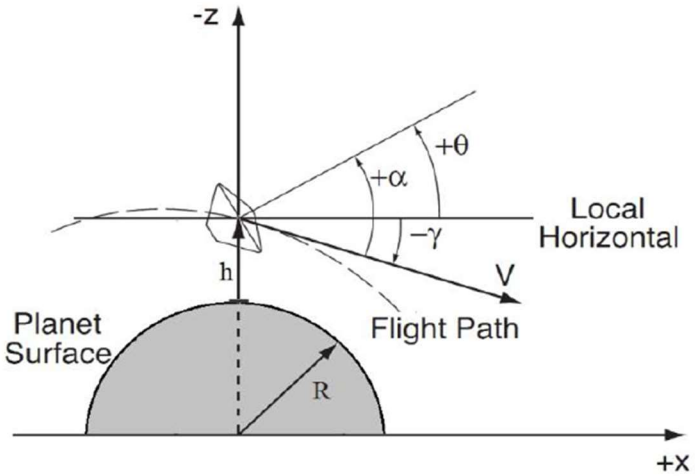

Figure 2: Reference Coordinate System [10].

Therefore, the following set of three equations describing the motion of the vehicle can be obtained [10]:

$$m\frac{dU_x}{dt} = q_\infty S C_D \tag{2}$$

$$m\frac{dU_z}{dt} = q_\infty S C_L - mg + m\frac{U^2}{r} \tag{3}$$

$$I\ddot{\theta} = q_\infty S D C_{m_\alpha}(\theta - \theta_0) + q_\infty S \frac{D^2}{2U}\left(C_{m_q} + C_{m_{\dot{\alpha}}}\right)\dot{\theta} \tag{4}$$

where I is the inertia moment, $\dot{\theta}$ is the pitch angular acceleration, q_∞ is dynamic pressure, S is the reference area, D is the reference diameter, U is the free stream velocity with its component U_x and U_z, m is the mass, C_L is the lift coefficient, g is the gravity acceleration, θ is the pitch angle and $\ddot{\theta}$ is the pitch angular acceleration. Equation 4 describes the motion of the model around his pitching axis. The coefficient C_{m_α} is the static coefficient, which can be known thanks to the static measurement of the pitching moment, whereas $C_{m_q} + C_{m_{\dot{\alpha}}}$ is the dynamic coefficient, also known as pitch damping sum, which is indicative of the dynamic stability of the object. Several are the techniques to determine the pitch damping sum and for each technique the equations specialize depending on the method of evaluation. The following subsection will discuss one of the most used techniques in the dynamic damping evaluation throughout the literature, which is also the technique used in the present work, the Forced Oscillation Technique.

2.2 Forced Oscillation Technique

Dynamic wind tunnel testing with a forced oscillation setup generally uses an axial sting that measures forces and moments, as well as the rates of change of these parameters with respect to changing pitch angle or angle of attack. In order to capture the dynamic behaviour, a motor attached to the sting imparts a one-degree-of-freedom oscillatory motion to the vehicle at a wide range of frequencies and mode shapes. Sinusoidal motion is usually applied. The vehicle is inclined at a wide range of angles of attack and at each condition undergoes a series of small amplitude pitch oscillations. The damping response of the vehicle is measured as a function of pitch amplitude, angle of attack, Mach number and reduced frequency. Advantages of this technique are its direct measurement of the dynamic aerodynamic coefficients, controllability and repeatability, and its ability to match a wide range of reduced frequency parameters. Additionally, mass scaling is not generally required to obtain representative full-scale behaviour in the sub scale environment [11]. Drawbacks of forced oscillation tests are the sting effects on the damping, which largely affects the values of the pitch damping coefficient. Also, due to the nature of the test setup itself, only the average damping over a pitch cycle can be obtained [12].
Employing state-of-the-art Computational Fluid Dynamics (CFD) tools to predict dynamic stability has been attempted in recent years in an effort to build on the semi-empirical methods.
One of the most recent works on this subject can be found in [13], where the dynamic stability of the Orion capsule was analysed at two different subsonic Mach numbers (0.45 and 0.70) and a range of angles of attack (0° - 60°). The "damping-in-pitch" coefficients were determined by applying the forced-oscillation method through CFD techniques.

DOI: 10.13009/EUCASS2019-950

The predicted damping coefficients match well with those from the experiments, both in terms of magnitudes of the damping coefficients and the range of angles of attack for which the capsule is dynamically unstable.
The aim of this work is to apply CFD Forced Oscillation Technique to a deployable re-entry capsule, since it has shown good reliability in the literature. Specifically, the equations used to evaluate the dynamic stability of the capsule are based on the energy method [14], and are now briefly discussed.
The principle of the energy resolution consists in integrating the work absorbed by the system (corresponding to amplification) or dissipated (corresponding to damping) during one oscillation cycle. In fact, since the mechanical friction is not null in the driving system, some energy injection is always necessary to compensate the losses. The energy is injected by the power supply.
Depending on the loop direction, one can deduce if the system oscillations would be amplified or damped while subjected to free oscillations. The first case is represented by a counter clockwise loop associated to a dissipation of energy, whereas the second situation is associated to a clockwise loop associated to an input of energy, as it is shown in Figure 3. The general expression of the damping in pitch parameter is the following [15]:

$$C_{m_{\dot{\alpha}}} + C_{m_q} = \frac{\oint C_m d\theta}{\int_T \dot{\theta}^2 dt} \frac{2U}{D} \qquad \textbf{(9)}$$

where U is the speed of the capsule at a certain altitude during the re-entry phase, D is the reference diameter, Cm is the pitching moment coefficient and θ is the pitch angle. It can be deduced that the damping-in-pitch parameter (averaged over one oscillation cycle) can be computed by evaluating the integral of the pitching moment coefficient and the pitch angular velocity squared in one oscillation cycle.

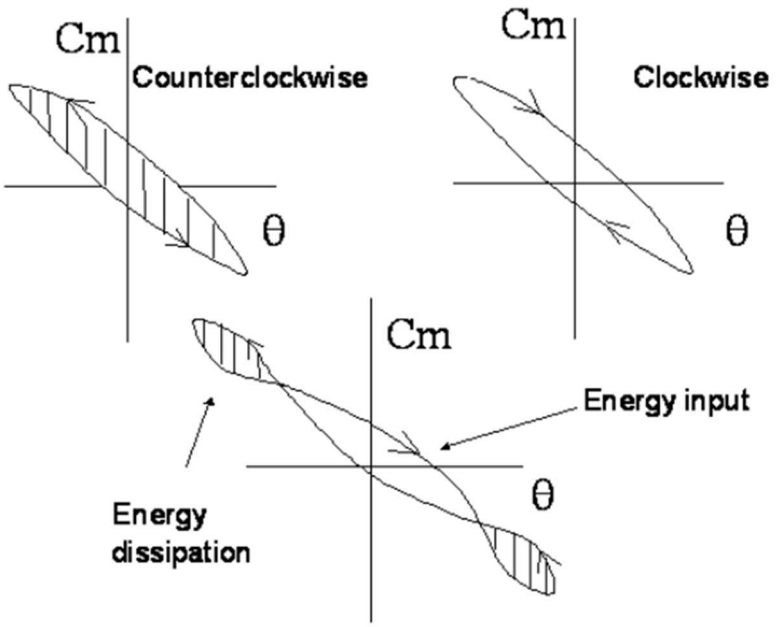

Figure 3: Energy method representation [15]

2.3 Geometry and meshing

The model used in the investigations is a capsule with a sphere-conical forebody heat shield. The cone semi-aperture angle ε is 45 deg. The body diameter D is 0.765 m, the position of centre of gravity (CoG) X_{CoG}, evaluated from the nose of the capsule, is 0.161 m, the distance of the shoulder from the nose L is 0.320 m, evaluated in the axial direction, and the nose radius is 0.328 m. The mass M is expected to be 12 kg and the reference surface S, estimated taking as reference length the body diameter D, is about 0.46 m^2.

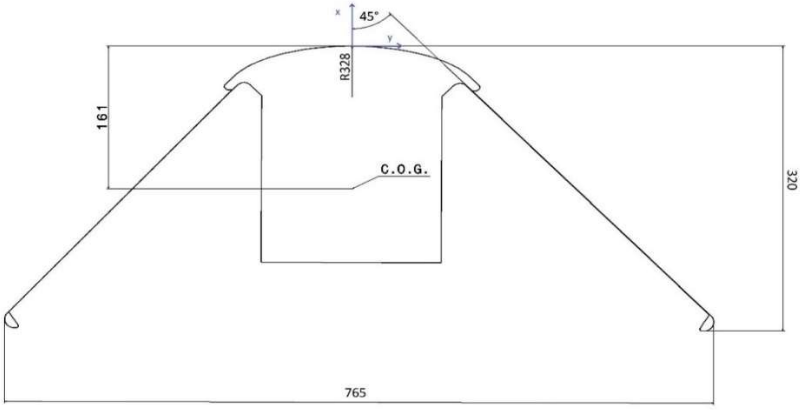

Figure 4: Capsule geometry. Dimensions are given in [mm]

The geometric characteristics are illustrated in Figure 4 and are summarized in Table 1.

Table 1: Geometric characteristics, mass and ballistic coefficient.

Body diameter, D	0.765 m
Position of centre of gravity, X_{CoG}	0.161 m
Maximum length, L	0.320 m
Nose Radius, Rc	0.328 m
Capsule semi-aperture angle, ε	45 deg
Reference surface, S	0.46 m^2
Mass, M	12 kg
Ballistic coefficient, β	23 kg/m^2

Figure 5 shows the CAD model. Clearly, only half capsule will be used for CFD simulation because of the body axial symmetry. Afterwards, the entire domain has been generated with CATIA software. Since our purpose is to determine dynamic stability by using the forced oscillation technique, a 3D domain is required for our case.
Specifically, the domain, also shown in Figure 5, is made of a typical 3D C-domain, within which a half sphere centred in the CoG of the capsule model is placed. Then, the capsule, placed inside the Sphere, has been subtracted through a Boolean Operation. The Sphere has a diameter equal to about five times the diameter of the capsule D. The C-domain, instead, has dimensions equal to about fifteen times the reference diameter D all around the capsule. This configuration of the domain allows the capsule, fixed to the sphere, to perform a rigid oscillatory rotation around its centre of gravity, in order to numerically reproduce the forced oscillation setup.

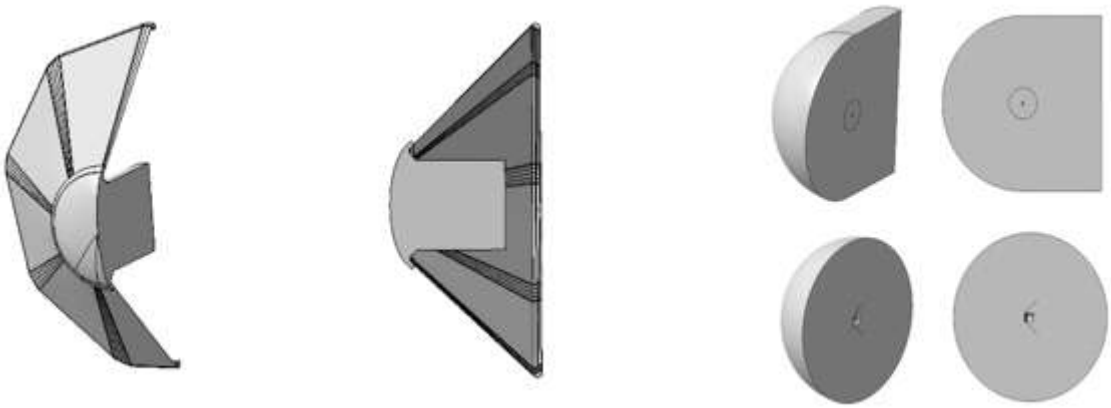

Figure 5: CAD model front and symmetry plane view (left). C-Domain cad model (right).

The domain CAD model have been imported in STAR-CCM+ to generate the mesh needed for the simulations. To provide a fast evaluation of the dynamic stability of a re-entry capsule, at the present stage a simple unstructured mesh has been developed and employed for both Eulerian and Turbulent simulations.

DOI: 10.13009/EUCASS2019-950

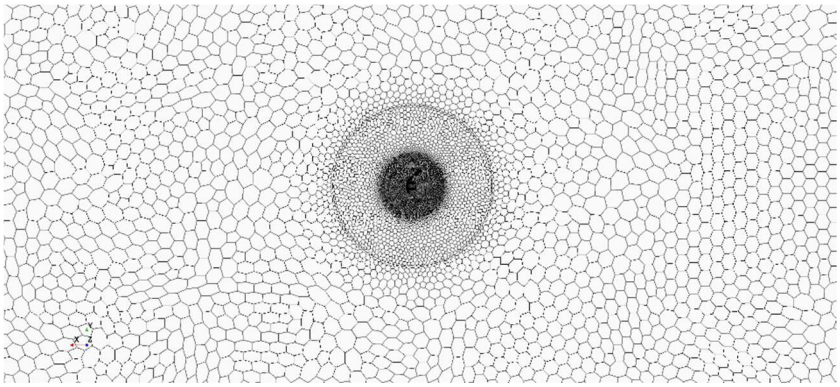

Figure 6: Polyhedral unstructured mesh.

Future developments will certainly include an improvement of the mesh to better take into account viscous effects. The mesh generated is shown in Figure 6. The base size is 0.2m, and the core volume has a growth rate of 1.3. Therefore, the cells far from the capsule, has greater dimensions, which is a benefit in terms of computational load. It must be pointed out that two different mesh operation have been necessary, because the domain consists in two different zone: C-domain, and Sphere. The surfaces in contact between these parts are treated as interface so that the solver would treat both Sphere and C-domain as a continuous fluid domain. The Sphere part was needed to simulate the oscillations of the capsule and so to apply the forced oscillation technique. In fact, it will rotate around its centre (that coincides with the CoG of the capsule) with a sinusoidal motion law.

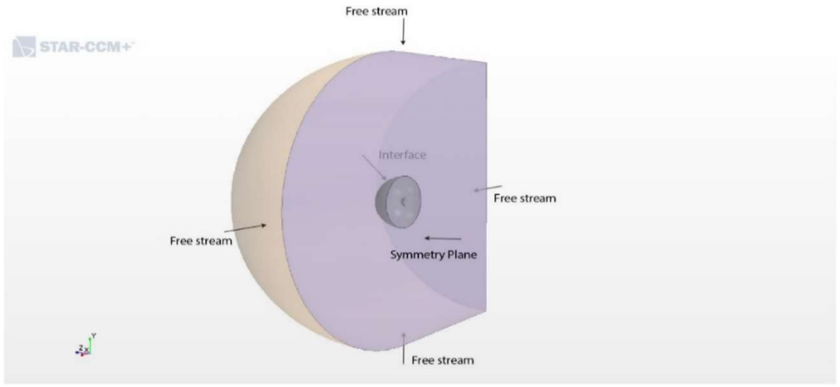

Figure 7: Simulation boundary conditions.

Moreover, around the capsule a volume control has been applied in order to better represent the fluid flow around the capsule and to better capture the shock-wave ahead of the capsule. All these operations led to a volume cell number of 502203.

2.4 CFD models and simulation conditions

The first simulation attempt has been a compressible inviscid one. Analysing the results, which are shown in the next section, it has been clear that Euler simulations were not able to capture properly the wake and the results were not reliable. Thus, a turbulence model has been introduced. Specifically, a k-ω turbulence model has been used. For both the models the boundary conditions, shown in Figure 7, are free stream, symmetry-plane, interface and wall. Free stream has been applied to all the faces of the fluid domain except for the plane of symmetry for both the C-domain and Sphere. Besides, there is the interface condition for the surfaces of Sphere and C-domain that are in contact and, obviously, the wall of the capsule. It must be pointed out that:

- The Spatial discretisation scheme is a 2nd order implicit integration of the equations.
- Time discretisation scheme is a 1st order implicit. The number of inner iterations is 200 and has been set in order to reach a good convergence of residuals and coefficients.
- Time step that has been chosen is 0.001 s, which ensures to be able to properly capture all the unsteady phenomena, considering the frequency chosen for the oscillations (1 Hz), and the frequency of the phenomena that has been found to be about 14 Hz [16].

In order to predict the dynamic behaviour of the capsule, the Sphere, which is a region within the fluid domain, must oscillate sinusoidally in time with a certain amplitude A and frequency f according to the following equation:

$$\theta = A \sin(2\pi f t) \quad \textbf{(10)}$$

Values of A and f of interest for the present analyses were selected based on the results of 6-DOF trajectory simulations carried out without taking into account damping dynamic derivatives. These analyses pointed out that the capsule is subjected to oscillations with a maximum amplitude of 10° and a frequency from 1 Hz to 10 Hz. Considering such results, it has been chosen to perform oscillations with a frequency of 1 Hz and with an amplitude equal to 2 deg, 5 deg and 10 deg. Furthermore, it has been estimated the natural pitching frequency of the capsule is 1 Hz one order of magnitude lower than the aerodynamic buffeting frequency.
In section 1.1 it is mentioned that the most critical part of the re-entry trajectory in the frame of dynamic stability is the transonic regime. Therefore, in order to predict the dynamic behaviour of the capsule, the conditions chosen for the simulations are the supersonic, transonic and subsonic one reached during re-entry. Specifically, two supersonic (M=3, M=2), two near transonic (M=1.2, M=0.8) and one subsonic (M=0.3) conditions have been selected. Then, considering the re-entry trajectory [9], density ρ, pressure p, temperature T and dynamic viscosity μ have been evaluated according to the standard atmosphere model US1976. Table 2 shows all the conditions selected.

Table 2: Selected conditions along the re-entry trajectory.

H (km)	M	$p*10^{-2}$(kg/m^3)	p (Pa)	T (K)	$\mu*10^{-5}$(Pa*s)
32.8	1.2	1.16	771	231	1.512
22.9	0.3	5.57	3520	219	1.449
30.9	0.8	1.61	1050	227	1.493
35.6	2	0.78	531	238	1.555

[a]Density, temperature, pressure and dynamic viscosity have been evaluated according to the standard atmosphere model US1976.

For each of the conditions gathered in Table 2, at least three simulations have been performed in the turbulent case varying the amplitude of the oscillation as mentioned in the previous subsection. In the inviscid case, instead, only the transonic condition (M = 1.2) with an amplitude A of 10 deg have been simulated. Only for the 1.2 Mach case the inviscid model has been used because it did not give reliable results, as it is shown in the next chapter. Moreover, for both the models, a frequency of 1 Hz has been set. In Table 3 all the simulation cases are shown and their results are discussed in Section 3.

Table 3: Simulation cases.

Model	Mach	A (deg)
Inviscid	1.2	10
Turbulent k-ω	0.3-2	2, 5, 10

3. Results

The first analysis being run is an unsteady compressible inviscid simulation with an oscillation amplitude of 10 deg and a frequency of 1 Hz. The flight condition is referred to a Mach number of 1.2 and the corresponding atmospheric quantities values are summarized in Table 2.
Four oscillation periods, hence four seconds, have been simulated. The moment coefficient evaluated with the respect to the CoG of the capsule as a function of the time and of the pitch angle is shown Figure 8. It is clear, by looking at the figures, that no information can be carried out from these data. Thus, a smoothing operation is needed. Specifically, the CM values are smoothed by using the "*smooth*" function in MATLAB. This function works by smoothing data using a specified filter method and span (a percentage of the total number of data points, less than or equal to 1). Good results are achieved using a span of 0.1 and a filter method called "*rloess*", a robust version of "*loess"* (local regression) that assigns lower weight to outliers in the regression and assigns zero weight to data outside six mean absolute deviations [17]. The result of these operations is also shown in Figure 9, where the smoothed CM is called "*CM clean"*.

DOI: 10.13009/EUCASS2019-950

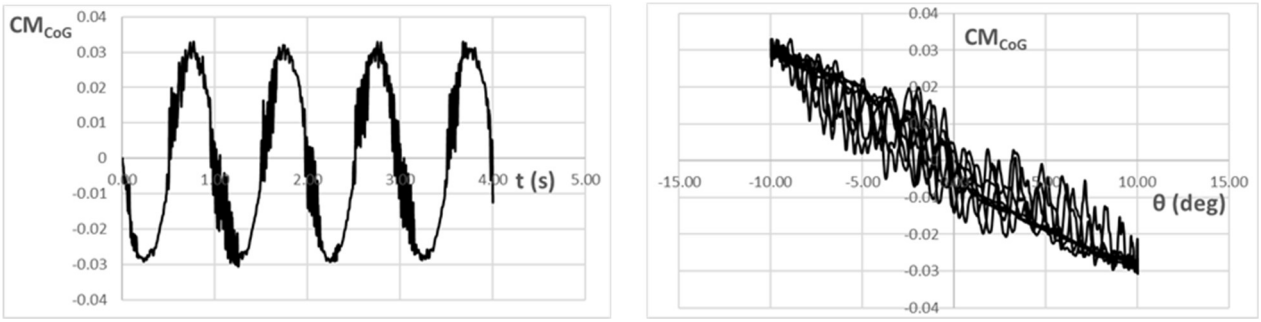

Figure 8: Four periods of the CM_{CoG} (black line) and of the smoothed CM_{CoG} (orange line) as a function of time (left). Four cycles of CM_{CoG} as a function of the pitch angle (right). Inviscid case.

The first thing that can be seen is the direction of the cycle, which is clockwise. Hence, the value of the damping sum is expected to be positive, which means that the capsule is dynamically unstable. Applying equation (9) the value of the pitch damping sum is:

$$\boldsymbol{Cm_{\dot{\alpha}} + Cm_q = 0.934\ (rad^{-1})}$$

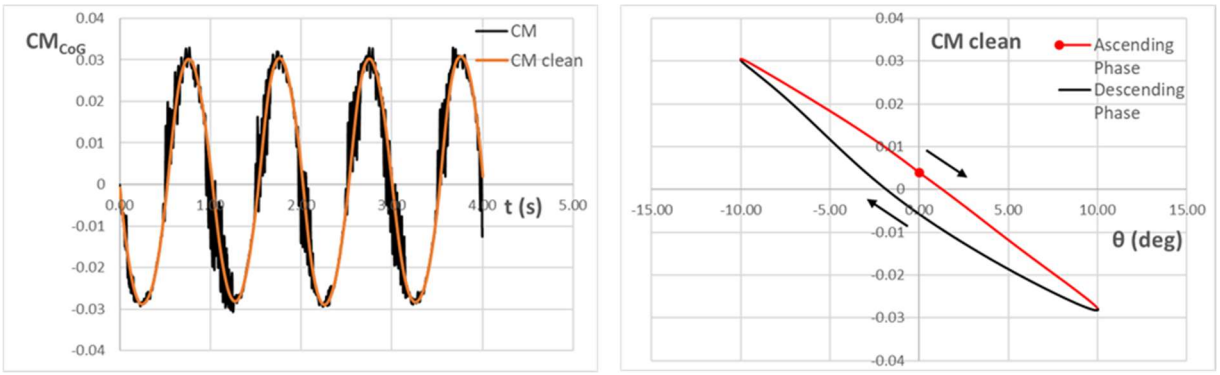

Figure 9: Four periods of the CM_{CoG} (black line) and of the smoothed CM_{CoG} (orange line) as a function of time(left). Cycle of CM clean in the ascending (red) and descending (black) phase of the oscillation. Direction of the cycle is also shown(right).

Thus, in this inviscid case, the capsule is dynamically unstable. Nevertheless, the highly oscillating CM profiles, shown in the previous figures, reveal the inviscid model poor capability to describe the phenomenon properly. This is also confirmed by the contours of velocity, shown in Figure 10, where it can be seen that the wake has not been captured correctly, suggesting that the result is not reliable.
In order to make a comparison with the inviscid case, the results of the Mach 1.2 turbulent simulation are presented. Figure 11 shows the CM_{CoG} as a function of the time (left) and pitch angle (right), respectively. The hysteresis cycles over the four period are narrow in this case as well. Therefore, an enlargement procedure is applied. The loop direction is counter-clockwise. Thus, the capsule is dynamically stable in this case, as can be confirmed by the sign of the average damping-in-pitch parameter

$$\boldsymbol{Cm_{\dot{\alpha}} + Cm_q = -0.163\ (rad^{-1})}$$

In Figure 12 the velocity contours over the second oscillation period are shown with a time span of 0.2 seconds carried out for the turbulent case. Within the contours all the main element of the flow structure around a blunt body are present: the shock wave ahead of the capsule, the Prandtl-Mayer expansion, recirculating region, recompression shock and the neck of the wake. Moreover, it can be immediately seen that the wake flow has been captured better in comparison to the inviscid case shown in Figure 10.

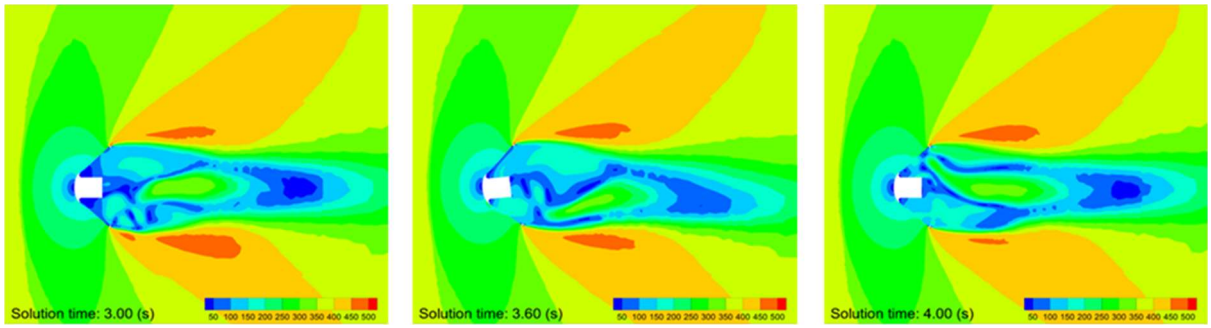

Figure 10: Velocity Magnitude (m/s) Contour at different time instants. Mach 1.2 inviscid case, A = 10 deg.

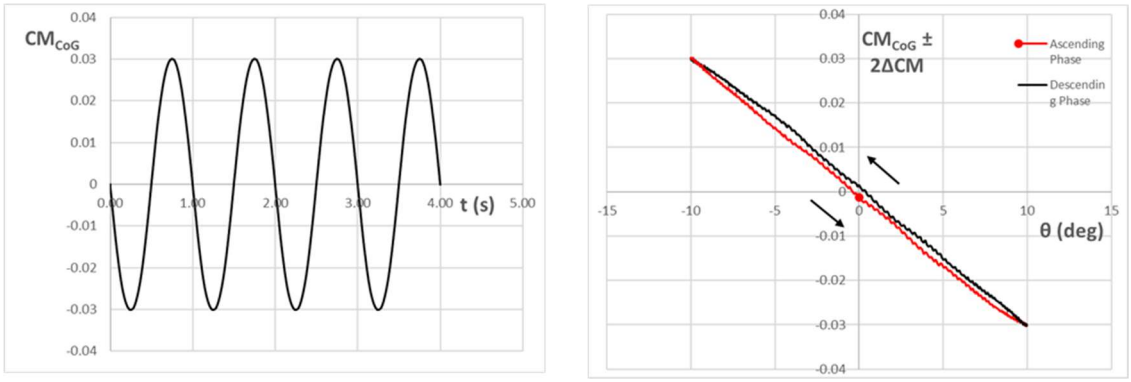

Figure 11: Four periods of the CM_{CoG} as a function of the time (left). Cycle of CM in the ascending (red) and descending (black) phase of the oscillation. For a better visualization of the cycle, the CM values have been altered with the ΔCM, which is equal to $\Delta CM=(CM_{up}-CM_{down})$, where CM_{up} and CM_{down} are maximum and minimum value of CM_{CoG} at the same angle θ. 2*ΔCM is added to CM_{up} and subtracted from $CM_{down.}$ (right). Mach 1.2 turbulent case, A=10 deg.

It must be pointed out that the wake follows the motion of the capsule and, in this motion, it has been observed a phase delay of the pressures before and after the capsule. This phenomenon is probably the main responsible of the hysteresis effect as can be confirmed by the study of Teramoto et al. [18].

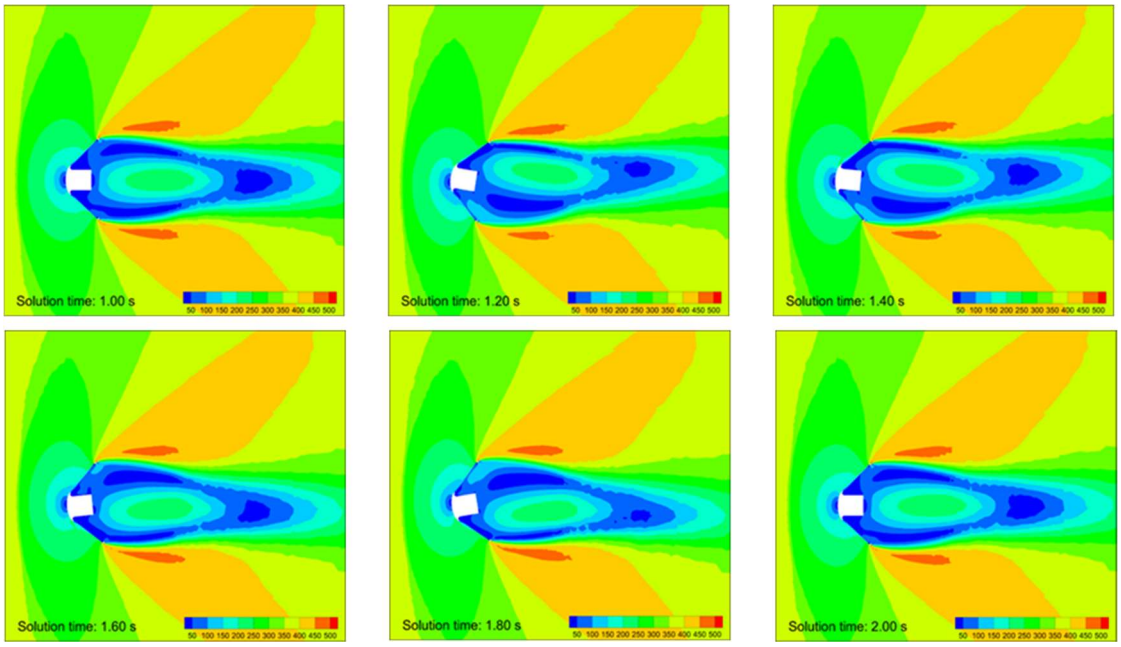

Figure 12: Velocity contours of the second period oscillation. Mach 1.2 turbulent case, A = 10 deg

DOI: 10.13009/EUCASS2019-950

The results of all the remaining simulations performed are summarised for brevity in Table 4 and are shown in Figure 14 as a function of Mach number and in Figure 14 as a function of pitch amplitude. The figures highlights the dynamic stability trend of the capsule. As can be seen, the oscillation amplitude has a considerable effect on the damping sum, as well as the Mach number.

Table 4: Simulation results.

Mach	**Amplitude**	$\boldsymbol{Cm_{\dot{\alpha}} + Cm_q}$	
1.2	2	0.627	**Unstable**
	5	0.059	**Unstable**
	10	-0.163	**Stable**
0.3	2	-0.116	**Stable**
	5	-0.203	**Stable**
	10	-0.213	**Stable**
0.8	2	0.007	**Unstable**
	5	-0.247	**Stable**
	10	-0.339	**Stable**
2	2	0.117	**Unstable**
	5	-0.366	**Stable**
	10	-0.618	**Stable**

At low amplitudes, namely 2 deg, the vehicle is unstable at all Mach numbers except for Mach 0.3, where the instability disappears. Increasing the amplitude, the pitch damping sum moves towards negative values leading to a dynamically stable behaviour of the capsule.

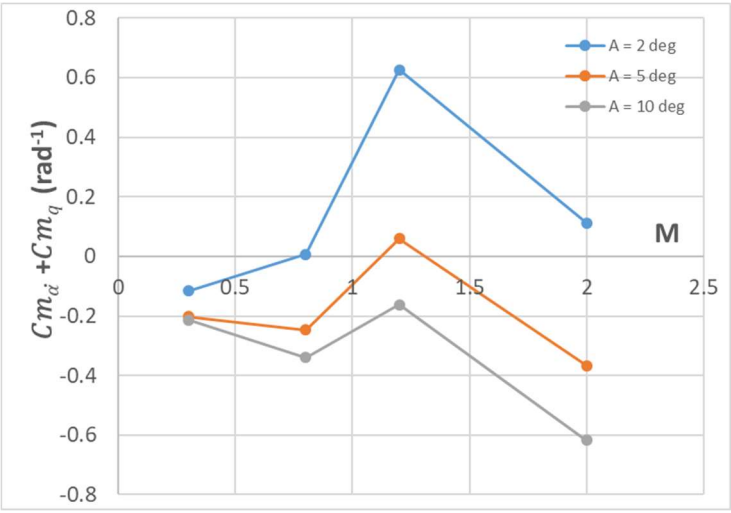

Figure 13 Damping sum as a function of Mach number at different oscillation amplitudes

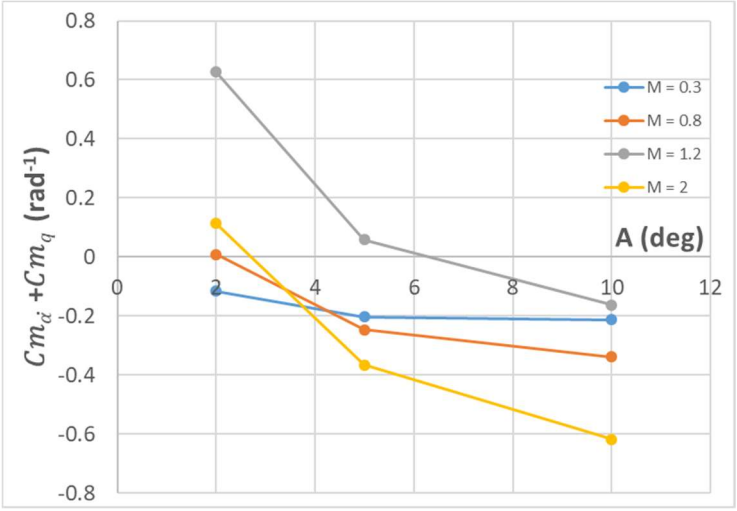

Figure 14: Damping sum as a function of oscillation amplitudes at different Mach numbers (right).

This behaviour is well-expected. Figure 15 and Figure 16 are taken from [19] and here shown for the sake of comparison. The first shows the effect of the pitch amplitude on the damping sum of the capsule Viking evaluated at Mach number 2.1 (cfr Figure 14). The latter shows the damping sum as a function of Mach number. As can be observed, the behaviour results of this work are perfectly in agreement with Viking ones, even though the instabilities are present at higher Mach number for Viking capsule.

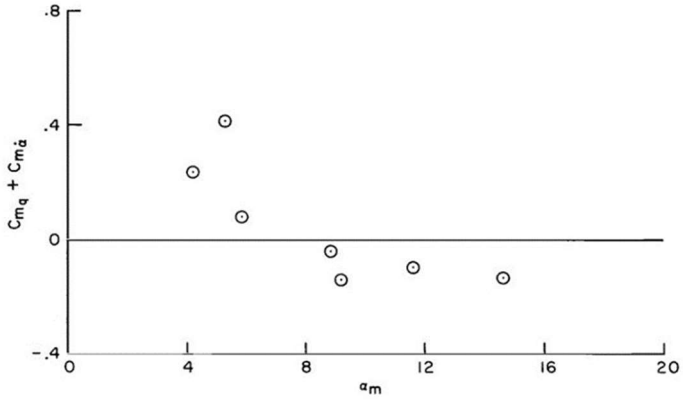

Figure 15: Pitch amplitude effect on the dynamic stability of Viking capsule. M = 2.1. [19]

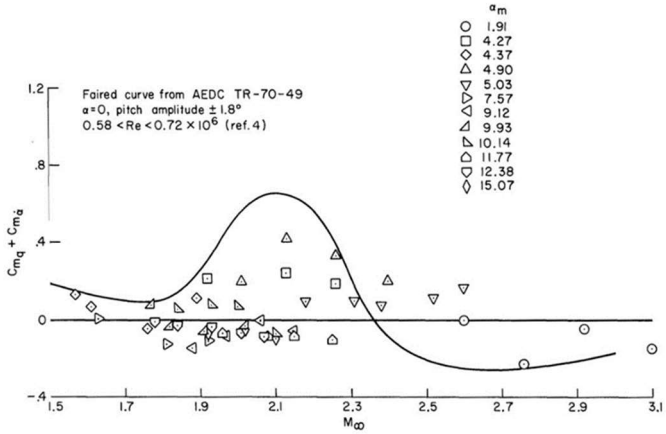

Figure 16: Variation of the dynamic stability with Mach number at different oscillation amplitudes of Viking capsule [19].

DOI: 10.13009/EUCASS2019-950

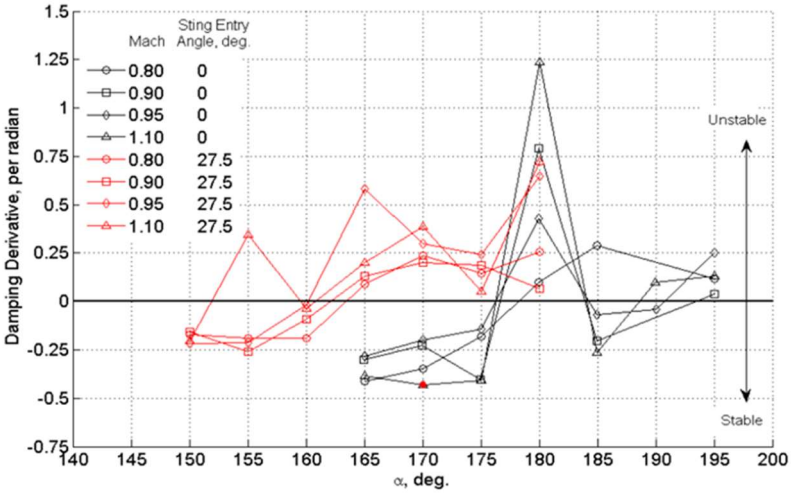

Figure 17: Orion crew module damping with sting entry angles of 0 deg and 27.5 deg. α=180 deg corresponds to 0 deg [11].

In Figure 17, referred to Wind Tunnel Forced Oscillation Test of Orion crew module and originally presented in [11] but reported here for comparison, is shown the effect of Mach number, of the sting and of the angle of attack on dynamic stability. In order to make a comparison with the present results, only the effect of Mach number at an angle of attack of 0 deg (α=180 deg corresponds to 0 deg) must be considered. Although in this case Orion capsule is always unstable, there is a peak of instability in the transonic regime.

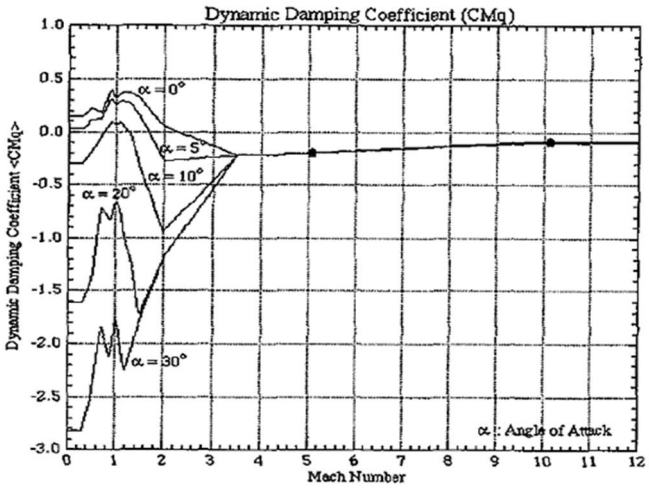

Figure 18: Dynamic Damping Coefficient vs. Mach Number Hayabusa capsule [20].

The same conclusions can be made by looking at the dynamic damping coefficient of Hayabusa capsule shown in Figure 18, taken from [20] and here shown for comparison, considering again only the case at 0 angle of attack. Besides, this behaviour is well-known in the literature and it is the reason why the effort to study dynamic stability on re-entry capsule is increased over the years.

4 Conclusions

The objective of this work was to study through CFD analysis, the aerodynamic stability of a deployable re-entry capsule with a 45° half-cone angle heat shield. In particular, the pitch damping sum ($C_{m_{\dot{\alpha}}} + C_{m_q}$) has been evaluated through the CFD forced oscillation technique, using the commercial solver STAR CCM+. The conditions analysed have been selected considering the suborbital re-entry trajectory of the capsule. First, analyses were conducted using an inviscid model, numerically solved by finite volume approach. The results have shown that the inviscid model has issues in describing the phenomenon of the dynamic instabilities, which, according to Teramoto et al., is related to the pressure lag between the forebody and the aftbody. In order to improve the capability to capture the wake and provide

more reliable results with respect to an inviscid simulation, Reynolds-Averaged Navier-Stokes equations, closed with the SST k-ω turbulence model were solved. The pitch damping sum of the capsule has been evaluated at four different Mach numbers (0.3, 0.8, 1.2 and 2) considering three different oscillation amplitudes (2 deg, 5 deg, 10 deg) at a frequency of 1 Hz. Values of amplitude and frequency of interest for the present study were selected based on the results of a preliminary six-degree-of-freedom trajectory analysis, carried out without taking into account damping dynamic derivatives. Results have been analysed in order to investigate the influence of Mach number and oscillation amplitude. At low amplitudes, namely 2 deg, the vehicle is unstable at all Mach numbers except for Mach 0.3, where the instability disappears. Increasing the amplitude, the pitch damping sum moves towards negative values leading to a dynamically stable behaviour of the capsule. Regarding the effect of Mach number, it is shown that there is a peak of instability around the transonic regime. Once the Mach number increases towards high supersonic values, the instability disappears, as well as in subsonic regime.
The predicted pitching behaviour has been compared with the available data in literature, showing a reasonably good agreement. The next step would be a validation of these results after the demonstration mission planned for the capsule chosen a reference case for this study [9]. Moreover, the results will be used as inputs for 6-DoF simulations of the capsule re-entry trajectories.

References

[1] D. L. Akin, «The ParaShield Entry Vehicle Concept: Basic Theory and Flight Test Development,» 1990.

[2] E. Venkatapathy, J. Arnold e I. e. a. Fernandez, «Adaptive Deployable Entry and Placement Technology (ADEPT): A Feasibility Study for Human Missions to Mars,» 2011.

[3] Cruz, J.R., Lingard e J.S., «Aerodynamic Decelerators for Planetary Exploration: Past, Present and Future,» in *Guidance, Navigation and Control Conference and Exhibit, AIAA 2006-6792*, 2006.

[4] R. W. Leonard, G. W. Brooks e H. G. McComb Jr, «Structural Considerations of Inflatable Reentry,» NASA Technical Note, 1960..

[5] R. Savino, E. Bassano and al., "IRENE - Italian Re-Entry Nacelle for microgravity Experiments," in *62nd International Astronautical Congress*, Cape Town, 2011.

[6] C. D. Kazemba, R. D. Braun, I. G. Clark e M. Schoenenberger, «Survey of Blunt Body Dynamic Stability in Supersonic Flow,» American Institute of Aeronautics and Astronautics, 2011.

[7] V. Carandente, G. Zuppardi e R. Savino, «Aerothermodynamic and stability analyses of a deployable re-entry capsule,» *Acta Astronautica,* vol. 93, pp. 291-303, 2014.

[8] G. Zuppardi, R. Savino e G. Mongelluzzo, «Aero-Thermo-Dynamic Analysis of a Low Ballistic Coefficient Deployable Capsule in Earth Re-Entry,» *Acta Astronautica,* vol. 127, pp. 593-602, 2016.

[9] A. Fedele e S. Mungiguerra, «Aerodynamics and flight mechanics activities for a suborbital flight test of adeployable heat shield capsule,» *Acta Astronautica,* vol. 151, pp. 324-333, 2018.

[10] M. Schoenenberger e E. M. Queen, «Limit Cycle Analysis Applied to the Oscillations of Decelerating Blunt-Body Entry Vehicles,» *RTO-MP-AVT-152,* 2008.

[11] D. B. Owens e V. V. Aubuchon, «Overview of Orion Crew Module and Launch Abort Vehicle Dynamic Stability,» in *AIAA 2011-3504*, 2011.

[12] C. H. Whitlock e P. M. Siemers, «Parameters Influencing Dynamic Stability Characteristics of Viking-Type Entry Configurations at Mach 1.76,» *Journal of Spacecraft and Rockets,* vol. vol. 9, n. no. 7, pp. pp. 558-560, 1972.

[13] A. S. Potturi e O. Peroomiany, «Dynamic Stability Analysis of the Orion Crew Module through Computational Fluid Dynamics,» in *46th AIAA Fluid Dynamics Conference*, Washington, D.C., 2016.

[14] S. Paris e Ö. Karatekin, «Experimental Determination of the Dynamic Derivatives of a Reentry Capsule in Transonic Supersonic Regime,» in *8th International Planetary Probe Workshop*, Portsmouth, Virginia.

[15] Ö. Karatekin, «Aerodynamics of a planetary entry capsule at low speeds,» VKI, PhD report, 2002.

[16] M. Iacovazzo, «Aerodynamic analysis of a low-ballistic coefficient deployable re-entry capsule,» Master's Thesis, 2013.

[17] MATLAB Documentation, Natick, MA: The MathWorks, Inc..

[18] S. Teramoto, K. Fujii e K. Hiraki, «Numerical Analysis of Dynamic Stability of a Reentry Capsule at,» *AIAA 98-4451 and AIAA Journal,* vol. vol. 39, n. no. 4, , pp. pp. 646-653, 2001.

DOI: 10.13009/EUCASS2019-950

[19] B. L. Uselton, T. O. Shadow e A. C. Mansfield, «Damping-in-Pitch Derivatives of 120-and 140-Degree Blunted Cones at Mach Numbers from 0.6 Through 3,» AEDC-TR-7049, 1970.

[20] K. Hiraki, Y. Inatani, N. Ishii, T. Nakajima e M. Hinada, «Dynamic Stability of Muses-C Capsule,» in *21st International Symposium on Space Technology, ISTS 98-d-33*, 1998.